JOURNAL OF MATERIALS SCIENCE 21 (1986) 1280–1288

Deposition of improved optically selective conductive tin oxide films by spray pyrolysis

I. S. MULLA, H. S. SONI, V. J. RAO, A. P. B. SINHA
Physical Chemistry Division, National Chemical Laboratory, Poona 411008, India

Antimony-doped SnO_2 films with a resistivity as low as 9×10^{-4} Ωcm were prepared by spray pyrolysis. Structural, electrical and optical properties were studied by varying the antimony concentration, film thickness and deposition temperature. About 94% average transmission in the visible region and about 87% infrared reflectance were obtained for antimony-doped SnO_2 films by a systematic optimization of the preparation parameters. As the best combination, an average transmission of 88% in the visible region and an infrared reflectance of 76% was possible for the doped SnO_2 films.

1. Introduction

Extensive work on SnO_2 and In_2O_3 films in the doped and undoped forms has been reported [1–14]. Various review articles are now available with up-to-date data on these materials [15–20]. From these studies it is well understood that the electrical conductivity, optical transparency in the visible region and the infrared reflectivity are inter-related. The increase in carrier concentration due to doping shifts the plasma edge to the shorter wavelength side, typically from 3.2 μm for pure SnO_2 films, to 1.3 μm for SnO_2 films doped with 3 at % Sb [21]. Such flexible tailoring makes the material suitable for its use in increasing the efficiency of the solar thermal conversion. It is for this reason that the films are transparent to visible radiation. Their plasma edge, as seen above, can be adjusted to somewhere between 1.5 and 2.5 μm, which is the region of the spectral separation between the solar radiation and the thermal radiation emitted by a body at a temperature typical for solar energy application. Therefore, these films are known as solar selective films.

Attempts have been made to prepare multilayered dielectrics [22], and microgrid structures [23] which produced good selectivity but these are complicated to prepare. Films prepared using sputtering techniques also give good selectivity [24, 25] but large-area deposition is difficult. On the other hand, only a few references are available where the selective films are produced using spray pyrolysis [26-28] which involves easily controllable process parameters of the spray pyrolysis technique. A systematic study was therefore carried out to determine the wavelength selective properties in SnO_2–Sb system. Wherever possible, attempts have been made to interpret the results.

2. Experimental details

To obtain better selectivity, one parameter involved is film morphology. Reports [29] from the literature indicate that only the sputtering technique produces the required morphology. However, a close control of the spraying parameters such as distance between the substrate and spray gun, uniformity of temperature throughout the substrate, etc., produces a film with the right morphology for obtaining selectivity [30]. The details of the formation process of such films are given below.

The tin oxide films were deposited on cleaned glass substrate (Microaid). The substrates were cleaned by boiling in 6 M analar reagent grade hydrochloric acid for 4 h, followed by boiling in distilled water for 0.5 h. Finally, the substrates were treated with benzene and then dried at 100° C for 2 h.

The undoped tin oxide films were then formed by the spray technique using 1 M anhydrous $SnCl_4$ (E Merck Darmstad) in dry ethanol. For doped SnO_2, the spraying liquid consists of 1 M $SnCl_4$ in ethanol to which varying volumes of 0.1M Sb_2O_3 in HCl were added to obtain different concentrations of antimony in the final composition. The concentration of antimony in various samples (designated by sample number) is given in Table I. The sprayer used was a conventional-type all-glass atomizer, where atomization was done using compressed air. A distance of 20 cm was maintained between the sprayer and the hot substrate. Each spraying period of 3 sec was followed by a 3 min interval. The depositions were carried out in the temperature range 300 to 600° C within an accuracy of ± 5° C. A furnace, 10 cm diameter and 25 cm high, with a proper thermal and electrical insulation was used. A refractory brick with a rectangular groove on top was then introduced. The larger thermal inertia of the brick helped in maintaining a uniform substrate temperature throughout the spray deposition.

Structural analysis was carried out using X-ray and electron diffraction techniques. Phillip's PW 1730 X-ray diffractometer with Cu$K\alpha$ radiation (λ = 1.54°) was used for phase identification, where diffracted X-ray intensities were recorded as a function of 2θ.

An electron diffraction study was carried out using a Finch-type camera, for which SnO_2 film was deposited simultaneously on rocksalt pellet and the glass substrate for recording electron diffraction

0022–2461/86 $03.00 + .12

TABLE I Optical and electrical properties as a function of antimony concentration in SnO_2 films

Sample no.	Mol % Sb in $SnCl_4$ (feed solution)	Properties of the deposited film		
		Infrared reflectance (%)	Visible transmittance (%)	Resistivity (Ωcm)
A_0	Undoped	30	88.0	6.0×10^{-3}
A_2	0.17	44	89.0	–
A_3	0.25	49	89.4	3.6×10^{-3}
A_4	0.30	54	90.0	2.4×10^{-3}
A_5	0.34	58	88.0	1.9×10^{-3}
A_6	0.38	61	88.0	–
A_7	0.42	65	89.0	1.4×10^{-3}
A_8	0.47	69	88.0	–
A_9	0.51	76	88.0	9.0×10^{-4}
A_{11}	0.59	70	86.7	1.1×10^{-3}
A_{12}	0.68	69	85.0	1.2×10^{-3}
A_{13}	0.77	–	82.7	–
A_{14}	1.01	66	81.5	1.3×10^{-3}
A_{15}	1.52	65	78.0	1.6×10^{-3}
A_{16}	2.52	53	71.0	2.2×10^{-3}
A_{17}	5.08	20	60.0	6.9×10^{-3}

patterns by transmission and reflection, respectively. The graphite ring pattern was used for calibration.

Resistivity measurements were carried using a four-probe method, in the temperature range 90 to 573 K under a constant vacuum of the order of 10^{-2} torr. Optical transmission measurements were carried out in the wavelength range 330 to 780 nm using the UV-VIS Specord Spectrophotometer. A blank undeposited part of the glass substrate was used as a reference.

The infrared reflectance was recorded as a function of wavelength (1 to 10 μm) by a Perkin Elmer double beam spectrophotometer model 221 using a reflectance attachment. A front-coated aluminium mirror was used as a reference for these measurements.

X-ray photoelectron spectra (XPS) were recorded with a VG scientific ESCA-3-MK II instrument at a base pressure of 10^{-8} to 10^{-9} torr with an Mg$K\alpha$ (1253.6 eV) radiation source. All spectra were recorded at 50 eV analyser pass energy, 4 mm entry slit, with 10^4 counts/sec, 0.1 sec time constant and 300 sec sweep time. The instrument was calibrated using the $Au4f_{7/2}$ peak (83.9 eV) as a standard.

3. Results and discussion

Fig. 1 shows the electron diffraction pattern (by transmission) for SnO_2 film which matches the SnO_2 structure, confirming the formation of SnO_2 film.

The effects of temperature of deposition on crystallographic structure by XRD for sample A_9 revealed that (i) no diffraction peaks were observed for films deposited at 350 and 400° C, (ii) low intensity peaks were observed for the films deposited at 450° C, (iii) sharp and intense peaks were observed for the film prepared between 500 and 550° C, indicating a higher degree of crystallinity for these films, and (iv) no peaks were observed for films deposited at 600° C, which can be correlated with softening of the glass. Therefore, films with various antimony concentrations were deposited at around 530° C.

XRD patterns (Figs. 2 and 3) for SnO_2 films deposited at 530° C with varying antimony concentrations suggested that up to 0.51 mol % Sb concentration (A_9), films show a better crystallinity which decreases progressively with increasing antimony concentration. The film with 5.0 mol % Sb concentration (A_{17}) shows a nearly amorphous nature. In our films, the reflection intensity for plane [2 0 0] is very prominent, while the [1 0 0] plane has been reported prominent in ASTM. This is indicative of some orientation of the film with the [1 0 0] plane parallel to the substrate. The observed orientation changed for the film sample S-34, where intensities of the [1 0 1] and [2 1 1] planes are enhanced. This suggests that the diagonal planes of type [1 0 1] are becoming parallel to the substrate.

Thin films of SnO_2 are prepared by the reaction

$$SnCl_4 + 2H_2O \rightarrow SnO_2 + 4HCl \qquad (1)$$

According to Arai [31] if this reaction is completed the

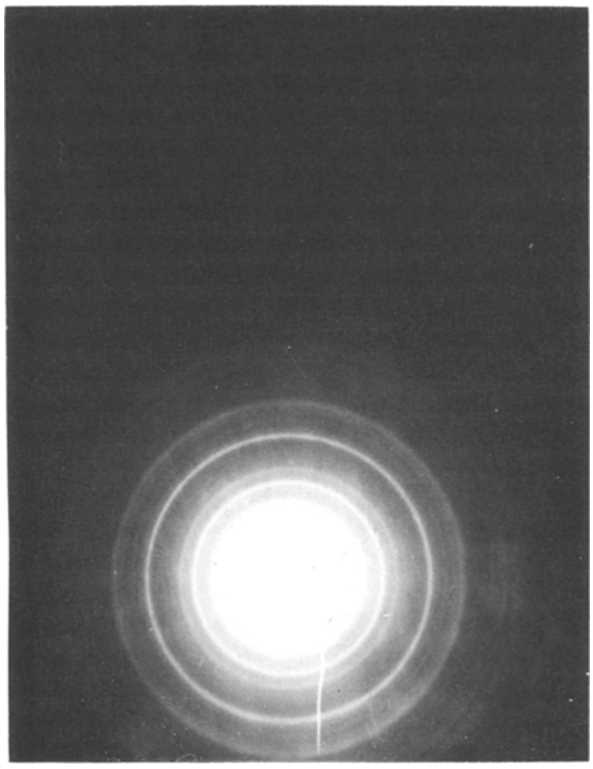

Figure 1 Electron diffraction pattern (transmission) for SnO_2 film.

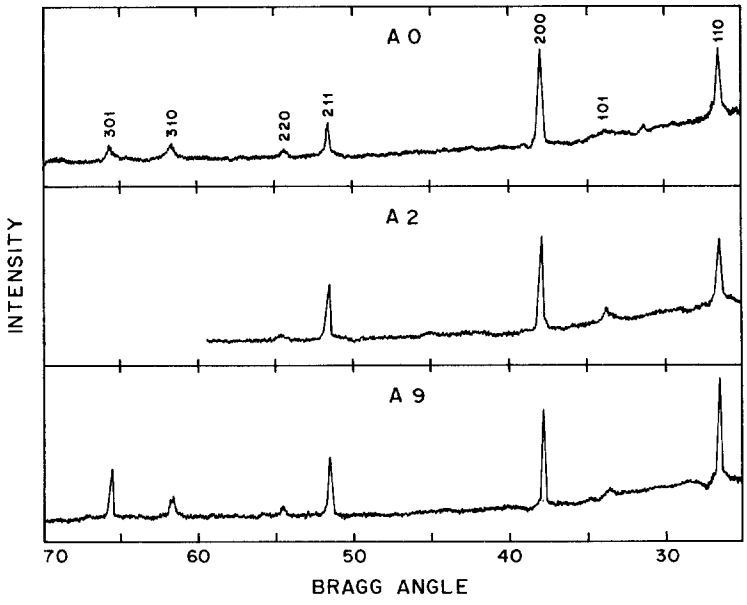

Figure 2 Diffraction intensity of various antimony concentrations in SnO_2 samples against 2θ for Cu$K\alpha$ radiation.

resulting SnO_2 would become an insulator. Since the films obtained by pyrolytic decomposition are conducting, the expected reactions are:

$$2SnCl_4 + 4H_2O \rightarrow SnO_2 + SnO + 7HCl \uparrow + \tfrac{1}{2}O_2 \uparrow + \tfrac{1}{2}Cl_2 \uparrow + \tfrac{1}{2}H_2 \uparrow + e \quad (2)$$

$$2SnCl_4 + 4H_2O \rightarrow SnO_2 + SnO + 8HCl \uparrow + \tfrac{1}{2}O_2 \uparrow + 2e \quad (3)$$

Therefore, the conductivity of undoped SnO_2 is attributed to a combination of chlorine ion and oxygen vacancies which result from incomplete decomposition of $SnCl_4$ and incomplete oxidation of the films. These defects are considered to be electron donors. We prepared SnO_2 films between 400 and 550° C by spray pyrolysis of $SnCl_4$; this method is known to produce oxygen vacancies and as the starting solution is $SnCl_4$ (and Sb_2O_3 dissolved in HCl), chlorine contamination is also expected. In fact, XPS indicated the presence of chlorine. So the low resistivity, $\varrho = 6 \times 10^{-3}$ Ωcm obtained for undoped SnO_2 film is attributed to the above defects. Oxygen vacancies forces equal the number of Sn^{4+} to reduce to Sn^{2+}

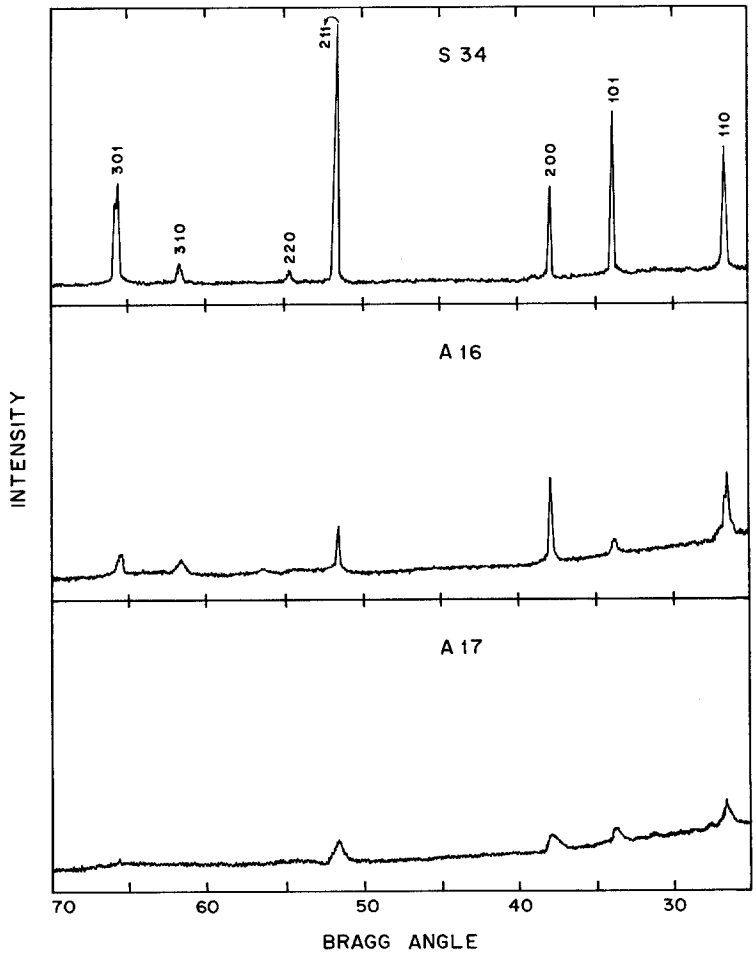

Figure 3 Diffraction intensity of various antimony concentrations in SnO_2 sample against 2θ for Cu$K\alpha$ radiation.

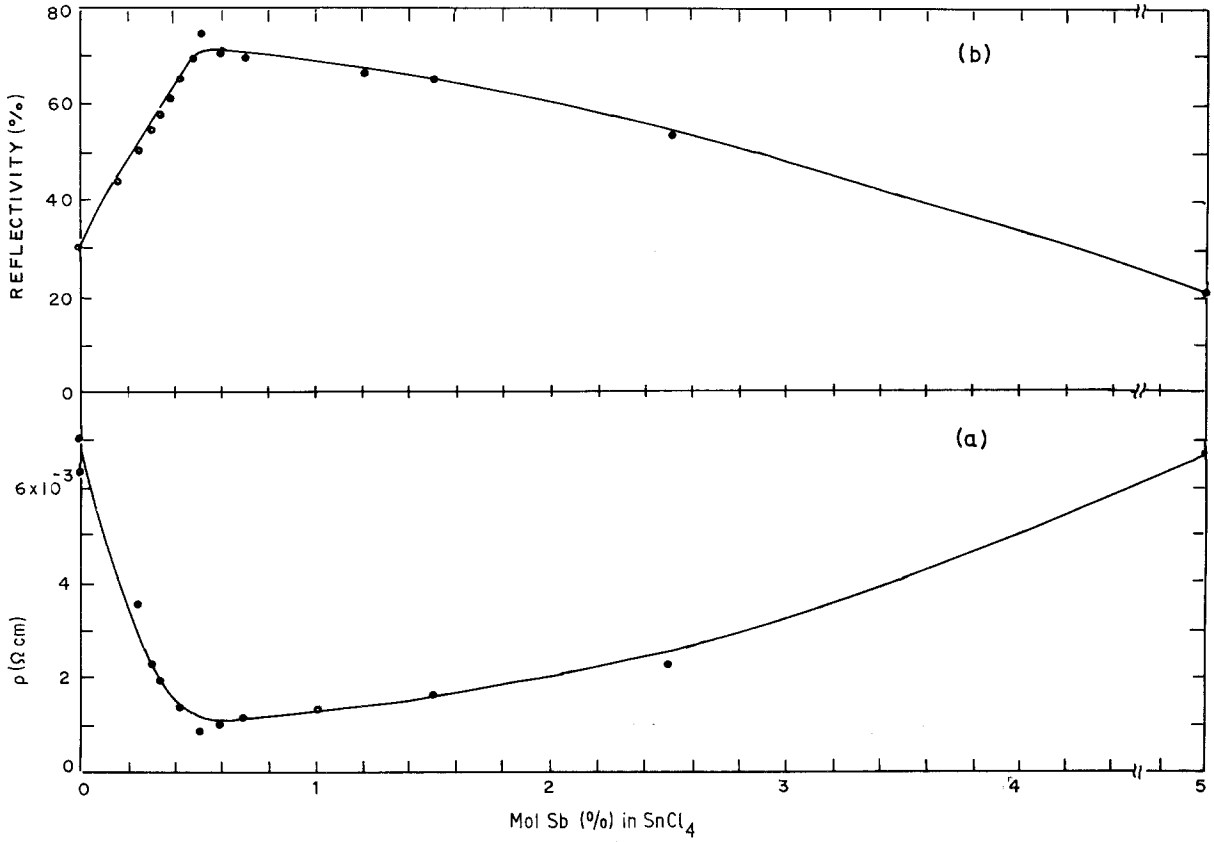

Figure 4 Variation of (a) resistivity, ϱ, and (b) reflectivity (%) as a function of antimony concentration in $SnCl_4$ feed solution.

which forms donor levels just below the bottom of the conduction band. However, at present we have no definite evidence for the presence or absence of Sn^{2+} states in our films. The activation energy calculated for SnO_2 films is in the range of 0.008 to 0.02 eV indicating the shallow levels.

On doping with antimony these SnO_2 films show a decrease in resistivity (Fig. 4). The decrease in resistivity is due to the substitution of Sn^{4+} by Sb^{5+} as their ionic radii are matching (Sn^{4+} 0.071 nm and Sb^{5+} 0.065 nm). It is observed that this substitution increases carrier concentration and thereby decreases resistivity. We observed the lowest resistivity $\approx 9 \times 10^{-4}$ Ωcm for the sample with 0.51 mol % Sb, while in the literature, the lowest reported is 2.3×10^{-3} Ωcm [32]. For this resistivity the source of antimony ion was from antimony chloride. In the present film, however, the source of antimony ion is from Sb_2O_3 dissolved in HCl. Therefore, the lower resistivity obtained for the present film may be due to the formation of some oxychlorides in the solution which in turn changes the final oxidation state of antimony [33]. The films with the lowest resistivity also show the highest crystallinity (Fig. 2, A_9). Therefore, besides a high carrier concentration due to antimony, the mobility of these carriers is also expected to be higher. With further increase in the antimony concentration in the SnO_2 film (from 0.51 mol % onward) the resistivity of the films begins to increase. The X-ray diffraction pattern showed a progressive decrease in the crystallinity with increasing antimony concentration. This is because antimony is one of the glass formers [34]. The decreased crystallinity causes disorders and thereby decreases mobility. The increase in resistivity with increase in antimony concentration is also due to the fact that carrier density is decreased as indicated by XPS studies. XPS studies [35] of $Sb3d_{3/2}$ levels of our film with lower antimony concentration showed only one peak with a binding energy at 540 eV, while the film with an antimony concentration of more than 2.5 mol % Sb showed an asymmetrical peak. This was resolved into two peaks. The binding energy values for these were close to those given for the mixed valence compound, Sb_2O_4. This showed that at higher antimony concentrations, part of the antimony was present as Sb^{3+} which caused an auto compensation: it acted as an electron trap and had removed electrons generated by Sb^{5+}.

Figs. 5a and b show the variation in the resistivity with temperature over the range 93 to 537 K. No appreciable change in resistivity is observed for doped and undoped SnO_2 films up to 400 K indicating that the charge carriers are ionized even at 93 K. However, beyond 400 K an irreversible decrease in resistivity is observed for SnO_2 films (not shown) and the films doped up to 0.42 mol % Sb (Fig. 5a, $A_{3\text{-}4\text{-}5\text{-}7}$). When annealed in an oxygen atmosphere, resistivity of these films again increased and the original resisitivity was almost achieved. The irreversible decrease in resistivity is, therefore, attributed to the desorption of oxygen from the grain boundaries resulting in a lowering of the barrier height and an increase in the mobility.

However, for films with a doping range from 0.5 to 0.8 mol % Sb is there no appreciable change in the resistivity over the entire temperature range (Fig. 5b, A_9 and A_{12}). The films in this region are degenerate. Such films can be represented by $Sn^{4+}_{(1-x)}Sb^{5+}_x\ e^-_x O^{-2}_x$ [36]. Presumably there are no Sn^{2+} ions and oxygen

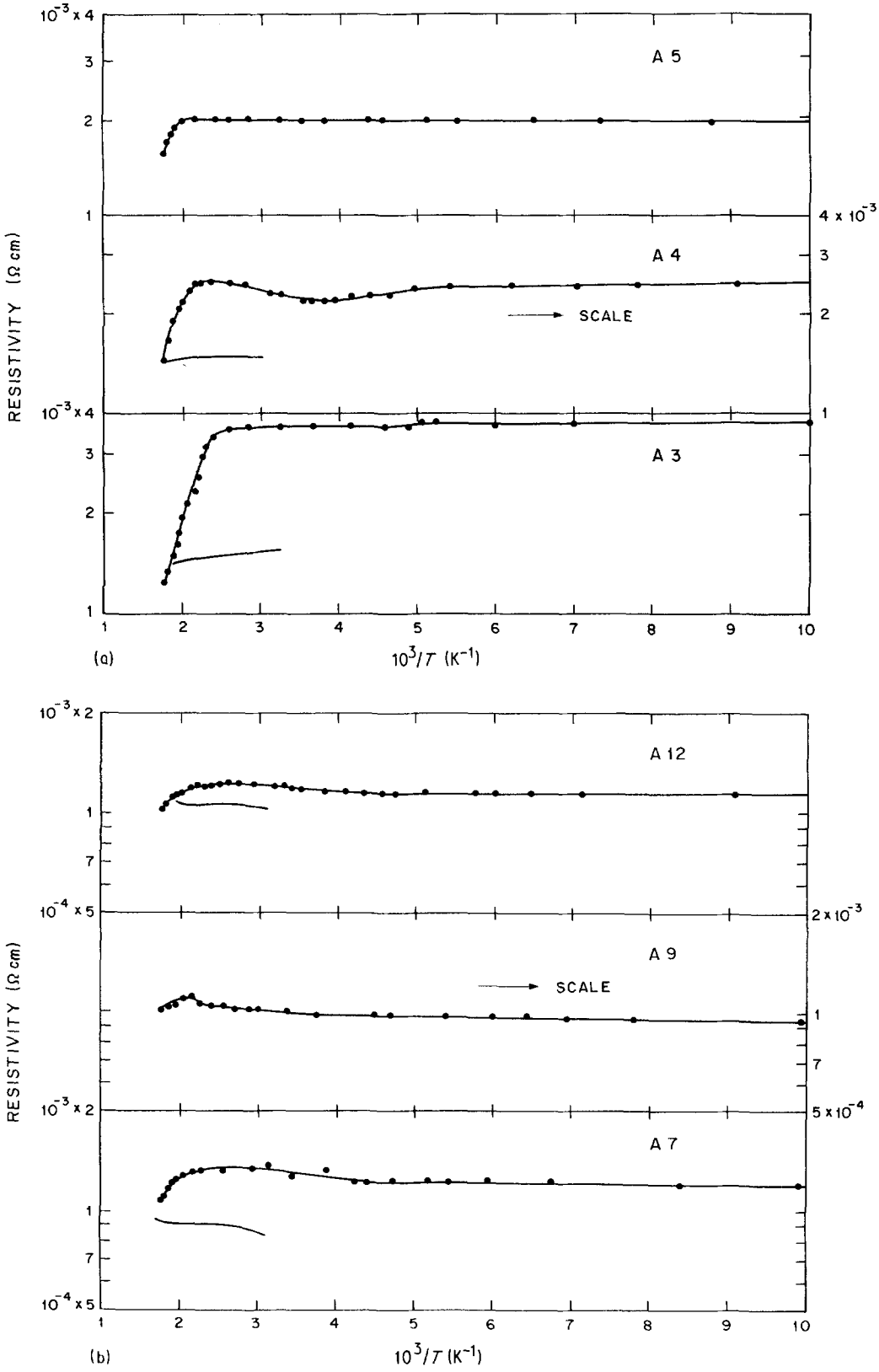

Figure 5 (a)Resistivity, ϱ, plotted against inverse temperature for various antimony-doped SnO_2 films. (b) Resistivity, ϱ, plotted against inverse temperature for various antimony-doped SnO_2 films.

vacancies. These films do not exhibit a change in resistivity with temperature, which can be attributed to the formation of an impurity band in the semiconductor [37].

It has been known that for SnO_2 films there is always a critical temperature of deposition at which the lowest resistivity is achieved. Poor crystallinity with higher resistivity has been found at lower deposition temperatures. Beyond the critical temperature, the reaction tends towards completion, thereby completing oxidation of the film, which in turn increases the resistivity of the film. We have seen 450° C to be the critical temperature for deposition of SnO_2 films. However, for antimony-doped SnO_2 film the observed results (Table II) indicate that by increasing the temperature of deposition the resistivity of the film decreases progressively. This may be attributed to the better incorporation of Sb^{5+} in the SnO_2 structure,

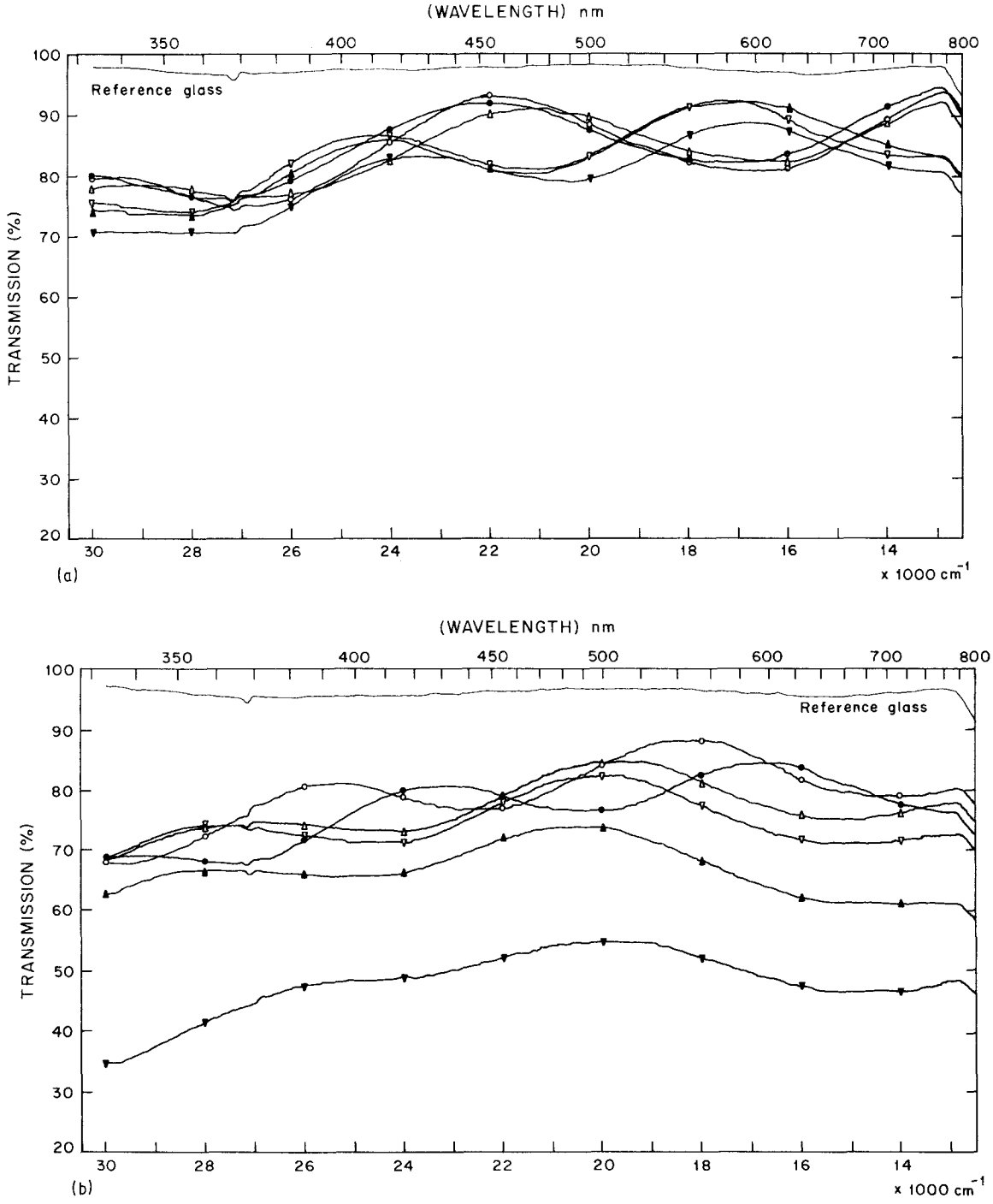

Figure 6 Per cent transmission of various antimony-doped SnO_2 films plotted against wavelength (nm). (a) ○; A_0, ●; A_3, △; A_5, ▽; A_6, ▲; A_9, ▼; A_{11}, (b) ○; A_{12}, ●; A_{15}; △; A_{14}, ▽; A_{15}, ▲; A_{16}, ▼; A_{17}.

and also the better crystallinity resulting at higher deposition temperatures.

The resistivity was measured at different film thicknesses, and an increase in resistivity was found with decreasing film thickness. A large drop in the mobility was observed by Van der Maesen and Witmer [38] for thickness below 100 nm. In addition to the expected causes, such as the presence of cracks, non-homogeneity and pore formation, this effect was attributed to the diffusion of impurities from the substrate or chemical reaction. It is observed that for a higher film thickness, the temperature dependence of resistivity is very small (< 40 ppm) which may be due to the mobility remaining independent of temperature in the

TABLE II Optical and electrical properties as a function of deposition temperature

Deposition temperature (°C)	Sample no.	Resistivity (Ωcm)	Infrared reflectance (%)	Visible transmittance (%)
350	T_1	5.2×10	7	87
400	T_2	9.9×10^{-2}	10	84
450	T_3	6.7×10^{-3}	23	84
500	T_4	1.2×10^{-3}	67	88
530	T_5	9.0×10^{-4}	76	87

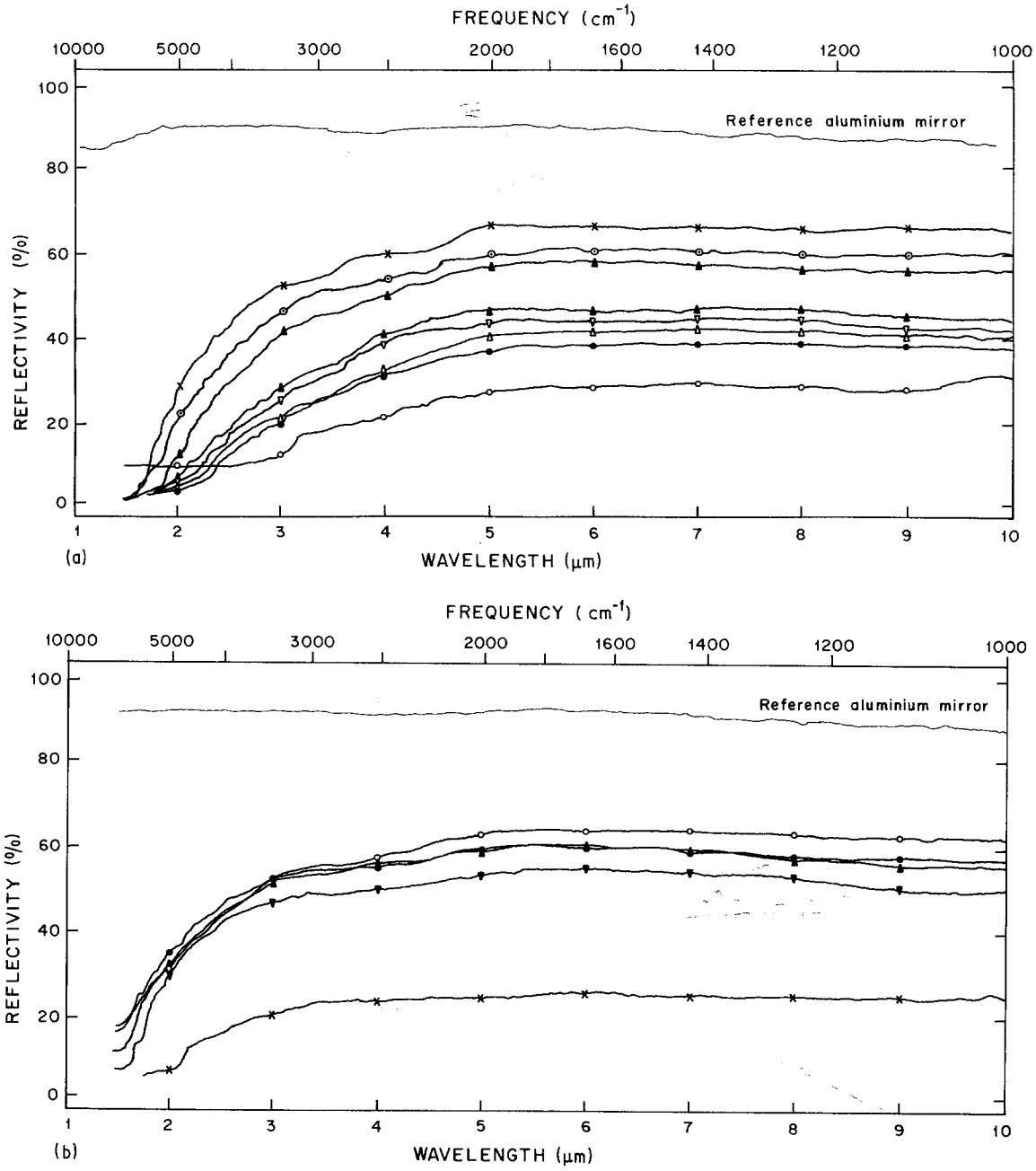

Figure 7 Variation of reflectivity with antimony concentration in SnO_2 film (a) ○; A_0, ●; A_2, △; A_3, ▽; A_4, ▲; A_5, ▼; A_7, ⊙; A_8, ×; A_9, (b) ○; A_{12}, ●; A_{14}, ▲; A_{15}, ▼A_{16}, ×; A_{17}.

thicker film. It could also be due to impurities diffusing in from the substrate or out to the substrate and neutralizing the doping effect of Sb^{5+}. The degenerate impurity band would disappear. The resistivity would rise, the impurity band width would shrink leading to a gap between the bottom of the conduction band and the impurity level. This would enhance the temperature effect.

The average transmission in the visible region as presented in Table I ranges from 57 to 93%, depending upon antimony concentration, thickness of the film and the temperature of deposition. A decrease in transmission is observed with increasing antimony concentration in the films. Higher antimony doping imparted blue coloration to the films which further reduces the transmission. The development of blue coloration is due to the high carrier concentration of antimony impurity. It is interesting to note that a high transmission peak in the visible region shifted after 0.35 mol % Sb doping. Up to 0.35 mol % Sb concentration the only smooth peak of the highest transmission (≈94%) was observed around 450 nm (Fig. 6a, A_0, A_3, A_5), while on increasing the antimony concentration above 0.35 mol % Sb, two distinct peaks were obtained around 420 and 580 nm (Figs. 6a and b, A_6 to A_{13}). For concentrations above 1.0 mol % Sb, only one peak at about 500 nm is observed (Fig. 6b, A_{14} to A_{17}) while at higher antimony doping, decreased transmission has been found. A shift in the high-transmission peak is also observed on changing the film thickness. The average transmission decreases with increased film thickness (Table III).

In general, in the visible region of the spectrum, the transmission is very high (high enough to observe interference fringes) which is due to the fact that reflectivity is low and there is no absorption due to transition of electrons from the valence band to the

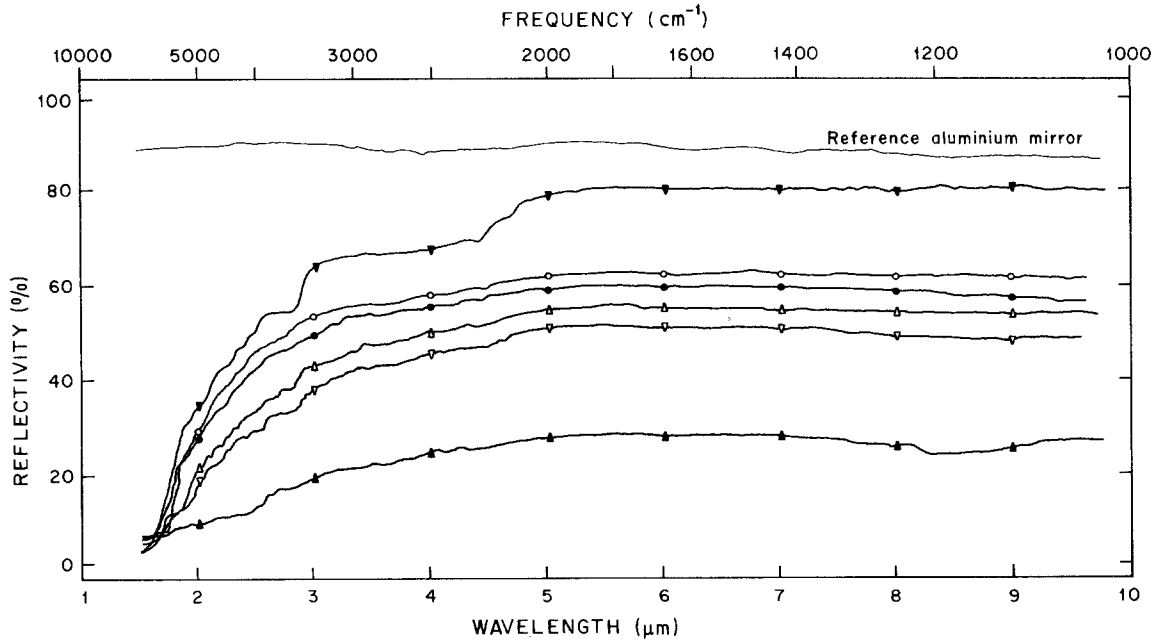

Figure 8 Effect of film thickness on infrared reflectivity, ○; D_1, ●; D_2, △; D_3, ▽; D_4, ▲; D_5, ▼; D_6.

conduction band. Owing to optical interference effects it is possible to maximize the transmission of a thin film at particular wavelengths. This is a useful technique to extend the transmission at the blue end of the visible spectrum, if the sheet resistance is low enough to meet the specification. We have observed as high as 95% transmission at wavelengths of 500 to 600 nm and resistivity as low as 9×10^{-4} Ωcm.

A systematic variation in infrared reflectivity is observed with change in resistivity of the film (Fig. 4) which in turn is controlled by antimony doping. Reflectivity is higher for the films with lower resistivity. Low resistivity films are degenerated and are highly crystalline. The high infrared reflectivity is attributed to the free carriers in these films. By carefully monitoring the spray parameters, it was possible to achieve the required morphology and film thickness and thereby 87% infrared reflectivity. However, transmission was decreased. Therefore, we optimized the process parameters to obtain the best combination as 88% average visible transmission and 76% infrared reflectance. Figs. 7a and b show the variation of infrared reflectance with variable antimony doping percentage in SnO_2 films at different wavelengths. The cut-off appears to be shifted towards the lower wavelength side with increasing antimony concentration (Fig. 7a) which is responsible for the increase in the free carriers. Further increase in the antimony concentration decreases the infrared reflectivity (Fig. 7b) which is due to the altered crystallographic order due to antimony addition, which reduces the carrier concentration and affects the reflection in the infrared range.

The optical properties of the polycrystalline films depend not only on their broad band semiconducting properties but also on the fact that the film thickness is one of the independent parameters to be considered. Table III shows the thickness dependence of infrared reflectivity. The infrared reflectivity increases up to a film thickness of 600 nm (Fig. 8). However, beyond this thickness no change in the infrared reflectivity was found. Upon increasing the deposition temperature, reflection in the infrared increases (Table II). It also increases upon annealing the film in a reducing (H_2:N_2) atmosphere (Table IV), while heating in air or nitrogen does not affect the reflectivity. It is also found that by increasing the moisture content, the resistivity of the film decreases and increases the infrared reflectivity (Table V). Kane *et al.* [39] observed that the presence of water vapour in the reaction gas stream lowered the refractive index of the tin oxide film. This may be the reason for increased infrared reflectivity with increased moisture content.

TABLE III Optical properties as a function of thickness

Sample no.	Thickness (nm)	Infrared reflectance (%)	Visible transmittance (%)
D_1	120	31	92
D_2	230	57	90
D_3	250	61	87
D_4	330	67	88
D_5	580	70	82

TABLE IV Effect of annealing in (H_2:N_2) 4:1

Sample no.	Infrared reflection (%)	
	Untreated	Treated
H_1	51.3	57.3
H_2	61.5	62.6
H_3	64.2	65.3
H_4	57.3	59.9

TABLE V Optical properties as a function of humidity

Sample no.	Moisture content	Infrared reflectance (%)
X_1	Dry air	57.0
X_2	Dry air	59.0
X_3	Air passed over water	64.5
X_4	Air passed through water	68.3

References

1. K. ISHIGURO, T. SASAKI, T. ARAI and I. IMAI, *J. Phys. Soc. Jpn.* **13** (1958) 296.
2. R. L. WEIHER and R. P. LEY, *J. Appl. Phys.* **37** (1966) 299.
3. H. K. MULLER, *Phys. Status Solidi* **27** (1968) 723.
4. O. V. VOROB'EVA and T. F. POLUROTOVA, *Ijv. Akad. Nauk USSR* **7** (1971) 206.
5. C. G. FONSTAD and R. H. REDICKER, *J. Appl. Phys.* **42** (1971) 2911.
6. H. KIM and H. A. LAITINEN, *J. Amer. Ceram. Soc.* **58** (1975) 23.
7. A. G. SABNIS and L. D. FEISAL, *J. Vac. Sci. Technol.* **14** (1977) 865.
8. R. H. BUBE, *J. Appl. Phys.* **49** (1978) 304.
9. E. LEJA, J. KORECKI, K. KROP and K. TOLL, *Thin Solid Films* **59** (1979) 147.
10. R. POMMIER, C. GRIL and J. MARUCCHI, *ibid.* **77** (1981) 91.
11. G. FRANK, E. KAUER and H. KOSTLIN, *ibid.* **77** (1981) 107.
12. K. B. SUNDARAM and G. K. BHAGWAT, *J. Phys. D.* **14** (1981) 333.
13. H. S. SONI, S. D. SATHAYE and A. P. B. SINHA, *Ind. J. Pure Appl. Phys.* **21** (1983) 197.
14. B. J. BALIGA and S. K. GANDHI, *J. Electrochem. Soc.* **123** (1976) 941.
15. Z. M. JARZEBSKI and J. P. MARTON, *ibid.* **123** (1976) 199C.
16. *Idem, ibid.* **123** (1976) 299C.
17. *Idem, ibid.* **123** (1976) 333C.
18. C. M. LAMPERT, *Sol. Energy Mater.* **6** (1981) 1.
19. J. C. MANIFACIER, *Thin Solid Films* **90** (1982) 297.
20. K. L. CHOPRA, S. MAJOR and D. K. PANDYA, *ibid.***102** (1983) 1.
21. E. SHANTHI, V. DUTTA, A. BANERJEE and K. L. CHOPRA, *J. Appl. Phys.* **51** (1980) 6243.
22. J. C. C. FAN, F. J. BACHNER, G. H. FOLEY and P. M. ZAVRACKY, *Appl. Phys. Lett.* **25** (1974) 693.
23. D. PRAMANIK, A. J. SIEVERS and R. H. SILSBEE, *Solar Energy Mater.* **2** (1979) 81.
24. D. B. FRASER and H. D. COOK, *J. Electrochem. Soc.* **119** (1972) 1368.
25. R. P. HOWSON and M. I. RIDGE, *Thin Solid Films* **77** (1981) 119.
26. M. JOHN BLOCHER Jr, *ibid.* **77** (1981) 51.
27. J. C. MANIFACIER, J. P. FILLARD and J. M. BIND, *ibid.* **77** (1981) 67.
28. G. BLANDENET, M. COURT and Y. LAGARDE, *ibid.* **77** (1981) 81.
29. H. W. LEHMANN and R. WIDMER, *ibid.* **27** (1975) 359.
30. I. S. MULLA, MSc thesis University of Poona (1981).
31. T. ARAI, *J. Phys. Soc. Jpn.* **15** (1960) 916.
32. J. KANE, H. P. SCHWEIZER and W. KERN, *J. Electrochem. Soc.* **123** (1976) 270.
33. M. RAMANUJAM and D. B. GHARE, *J. Ind. Inst. Sci.* **58** (1976) 254.
34. A. F. CARROLL and L. H. SLACK, *J. Electrochem. Soc.* **123** (1976) 1889.
35. I. S. MULLA, V. J. RAO, H. S. SONI, S. BADRINARAYANAN and A. P. B. SINHA, in preparation.
36. C. A. VINCENT, *J. Electrochem. Soc.* **119** (1972) 515.
37. V. K. MILOSLAVSKII and S. P. LYASHENKO, *Opt. Spectrosc.* **111** (1960) 455.
38. F. VAN DER MAESEN and C. H. M. WITMER, Proceedings of the 17th International Conference on the Physics of Semiconductors, Paris (1964) 1211.
39. J. KANE, H. P. SCHWEIZER and W. KERN, *J. Electrochem. Soc.* **122** (1975) 1144.

Received 12 April
and accepted 12 June 1985